

D17-39
N87-16759 258
44633

1986

NASA/ASEE SUMMER FACULTY FELLOWSHIP PROGRAM

MARSHALL SPACE FLIGHT CENTER
THE UNIVERSITY OF ALABAMA

THEORETICAL STUDIES ON THE MECHANICAL BEHAVIOR OF
GRANULAR MATERIALS UNDER VERY LOW INTERGRANULAR STRESSES

| | |
|-------------------------------|---|
| Prepared by: | Kenneth W. French, Jr., Ph.D. |
| Academic Rank: | Professor |
| University and Department: | John Brown University Department of Mechanical Engineering |
| NASA/MSFC: | |
| Laboratory: | Systems Dynamics |
| Division: | Atmospheric Sciences |
| Branch: | Fluid Dynamics |
| MSFC Colleague: | N. C. Costes, Ph.D. |
| Date: | August 15, 1986 |
| Contract Number: | NGT 01-002-099 The University of Alabama |

THEORETICAL STUDIES ON THE MECHANICAL BEHAVIOR OF
GRANULAR MATERIALS UNDER VERY LOW INTERGRANULAR STRESSES

by

Kenneth W. French, Jr.
Professor of Mechanical Engineering
John Brown University
Siloam Springs, Arkansas

ABSTRACT

The report describes the salient aspects of the theoretical modeling of a conventional triaxial test (CTC) of a cohesionless granular medium with stress and strain rate loading. Included are a controllable gravitational body force and provision for low confining pressure and/or very low intergranular stress. The modeling includes rational, analytic, and numerical phases, all in various stages of development.

This work is an extension of two previous summer's contributions to an ongoing project at NASA/MSFC and with contractors at the University of Colorado. Hence, this report builds strongly on the base of those from 1984 and 1985. The experimental culmination of the project will be performed in a mid-deck locker on a future Space Shuttle Flight. The numerical evolutions of theoretical models will be used in final design stages and in the analysis of the experimental data.

In this the experimental design stage, it is of special interest to include in the candidate considerations every anomaly found in preliminary terrestrial experimentation. Most of the anomalies will be eliminated by design or enhanced for measurement as the project progresses. The main aspect of design being not the physical apparatus but the type and trajectories of loading elected. The major considerations that have been treated are; appearance and growth of local surface aberrations, stress-power coefficients, strain types, optical strain, radial bead migration, and measures of rotation for the proper stress flux.

ACKNOWLEDGEMENTS

It has been very stimulating to serve the Fluid Dynamics Branch for a third summer. In spite of being kept abreast of the activities by phone during the "offseason", the strobe effect greatly enhances the amazing progress made by the Costes Team. It is a pleasure to see my colleague, Dr. N.C (Nick) Costes guide his team through various obstacles toward the culmination phase. I am grateful that Nick manages to incorporate my efforts into his overall goals.

In a program whose members individual requirements vary so widely as to be almost unique, Dr. L.M. Freeman has shown an astonishing flexibility and has provided excellent leadership with perfect attention to detail and beyond that to hospitality. Our new NASA leaders, Dr. Fred Speer and Ernestine Cothran brought a freshened vigor to the mapping of academic talents onto NASA Goals. The new team also has the promising prospect of establishing longer range continuation of efforts than have been previously possible.

One measure of success for the summer for NASA's senior patron of granular mechanics will certainly be that there was neither any swinish acappellation nor subsequent discomfort.

CONTENTS

| <u>number</u> | <u>title</u> | <u>page</u> |
|---------------|---------------------------|-------------|
| [1] | INTRODUCTION | 1 |
| [2] | OBJECTIVES | 3 |
| [3] | JAUMANN QUANDARY | 4 |
| [4] | STRESS POWER | 8 |
| [5] | STRAIN DEFINITION | 10 |
| [6] | THIN SHELL CONSIDERATIONS | 12 |
| [7] | NUMERICAL APPROACHES | 17 |
| [8] | RESULTS & RECOMMENDATIONS | 19 |
| [9] | REFERENCES | 20 |

FIGURES

| <u>number</u> | <u>title</u> | <u>page</u> |
|---------------|-----------------------------|-------------|
| [1] | TYPICAL TRIAXIAL APPARATUS | 2 |
| [2] | EFFECTIVE LOADING DIAGRAM | 2 |
| [3] | RR STRESS FLUX | 6 |
| [4] | W* STRESS FLUX | 6 |
| [5] | THIN SHELL FAILURE PATTERNS | 16 |
| [6] | LENGTH SCALES CARICATURE | 14 |
| [7] | TYPICAL LENGTH SCALES | 14 |
| [8] | GRANULE MEMBRANE SHELL | 15 |
| [9] | SHELL CALCULATION | 15 |
| [10] | EFFECT OF IMPERFECTION | 15 |
| [11] | E-t VARIABLE | 15 |
| [12] | SPHERICAL CATASTROPHE | 14 |

INTRODUCTION

The 1980s seem to be the decade for the coming of age for advanced analysis in rheology and soil mechanics. They are quickly catching up to their simpler, faster developing sisters; fluid and structural mechanics. In the granular mechanics community there seems to be almost a rush to install the full results of rational modeling and large strain plasticity theory. Rates of stress and strain are being incorporated into constitutions, objectivity is demanded, stress power is accounted, and damage, memory, and fracture are actively courted. However, there is something grander about this whole development. The behavior of granular material has long escaped analytic capture for a very good reason; it exhibits a very complicated constitution. Granular materials have evaded analysis except in the very restricted local sense of using test coefficients in an interpolated analytic framework. Often even then a confining history must be specified. Further the dissimilarities among soil types is wondrously wide, to say nothing of the spectrum of man-made substances with discrete particles from elastic/brittle glass to polymeric types with memory.

The new models are immediately followed by computer analysis which by prediction enhances final design stages and which by correlation enhances the results of prototype and final experiments. Nevertheless as the lessons in turbulence in fluid mechanics and buckling in structural mechanics have shown, the progress with numerical analysis will still prove to be a frontier for many years.

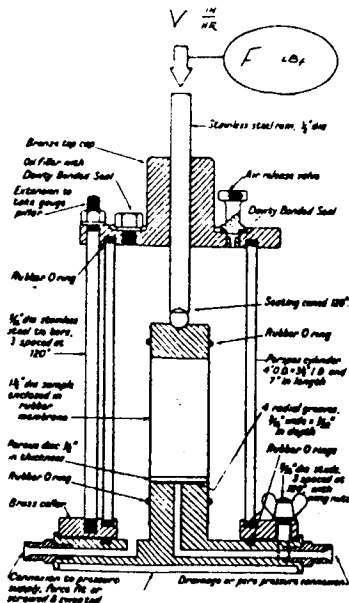
Whether the bevy of classical soil mechanics tests are thought of as studies of the behavior of infinite half-spaces of granular material or as a search of constitution by partial derivative or as preparation for the use of membranes for control of granular bulk; the influence of gravity body force is crucial to a full understanding. Our human intuition is built on experiences with granular media under the domination of gravity. Outside that realm there are precious few (albeit extremely interesting and crucial) cases and those highly transient. Separation by flow of multicomponent saturated river beds, liquefaction in quicksand or under earthquake or other strong cyclic loading, cyclic mobility deformations; but at best these are transient snapshots of low intergranular stress behavior.

There is also the very interesting prospect of the granule being the ideal form for storage of bulk material in zero-g. The underlying reason being its ability to exhibit high or low frictional forces. Unfortunately, this characteristic is strongly inhibited by strong gravitational forces which confine the granules; hence, soil liquefaction is a rarity on earth which does not sadden civil engineers.

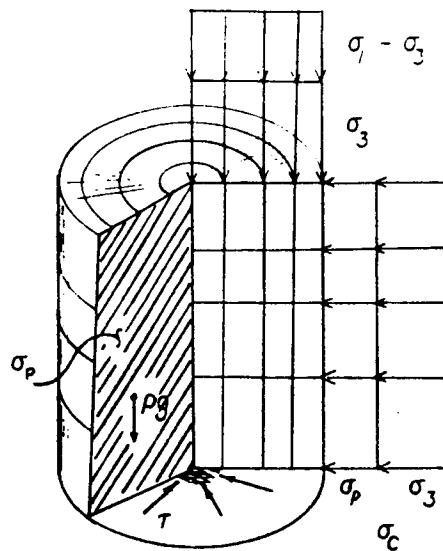
Vibratory transport with fluxes of discrete masses has been employed commercially for many years. This in combination with an oscillating confining pressure has potential; the former to move the latter to act as a check valve. In space a double membrane container with pressure control of the intermembrane region and vacuum or pressure control to the inner region would allow behavior ranging from near fluid to tremendously frictional and hence either pumping or the retention of the integrity of an almost arbitrary shape. Therefore either bulk storage or peristaltic transport are realizable within the same containment. That is a granular material does not have the high bonding of a frozen solid nor is it dominated by surface tension or vapor pressure typical to liquids.

The concept of a granular media as a 3-D fabric with noncatastrophic damage being done continuously by the loading represents perhaps the best thermodynamic view and keys on vision of stress-power. Ultimately this damage becomes particle crushing, shear banding, fabric fracture and if loading is strongly cyclic or containment small, cyclic mobility or liquifaction.

It is into this fascinating realm that the "Costes Team" commenced finding a niche in 1978. The particular geometry chosen is the classical triaxial test with provision for saturation draining and a variety of loading trajectories; see Figures 1 and 2. The following section will detail the exact position of this work in the general development of the ongoing project. The experimental culmination being Space Shuttle borne tests of a wide variety and the constitutive theory an unending frontier of discovery based on these better low intergranular stress results.



TRIAxIAL TEST
FIGURE 1



EFFECTIVE LOADING DIAGRAM

FIGURE 2

OBJECTIVES

The primary goal of this work is to provide theoretical modeling support for the Mechanics of Granular Media (MGM), activity with special direction toward the models for the conventional triaxial configuration with specimens of cohesionless spheroidal material. In this respect it is a true continuation of the past years' work.

The objectives of this work are to provide state of the art rational modeling, analysis within the precision required, and numerical support for the full range of constitutions and for anomalies outside the model. Typically the model is local, a differential continuum; the analysis is global, integral; and the numerical approach attempts both local and global approximations. It is necessary to explicitly include acceleration of gravity and mass density. The former for body force control and the latter for that as well as density sensitivity in the constitution and for tracking dilation.

One of the primary objectives is to confront the real boundary conditions of platen encroachment, membrane adjustment and penetration, and boundary shear stress power and to resign them to the constructions used in analysis. This is crucial; to relate all the statements of deformation and its time and space derivatives through all three theoretical phases. The careful, definitive statement of strain will permit a correct extension to the use of optically measured displacements on the cylindrical boundary. Preliminary calculations of the inherent experimental strain uncertainty are desirable to anticipate the necessary prediction level for the analytic and numerical phases.

The numerical objective is to provide a local version of the MICROFEM code that is fully interactive, specialized to a reasonable level of entry data, implemented with screen prompting and segregated from the FEM skeleton. A brief manual will be produced to guide operation and to document the flow of the code through subroutines so that modification can be made and behavior traced to its origin. This code should accommodate a variety of constitutive models, but be limited to a single solver and to the geometry, and loading trajectories envisioned for the culmination experiments. The FEM must reenter the constitutive model at every iteration and be fully sensitive to the boundaries of behavior internal to the stress space.

JAUMANN QUANDARY

A conference paper in 1981 showed that under certain conditions the combination of a Prager-Ziegler kinematic hardening rule with a Jaumann stress flux can cause an oscillatory stress-strain relationship. Figures 3 & 4 show some extreme and more mild forms of this oscillation; they are from Lee(82) and Dafalias(82) respectively. It is interesting to note that Lee et al were the editors of the conference at which the original paper was presented.

The conclusion of Lee(82) and Dafalias(82) and subsequently of Kioussis(86) was that the Jaumann stress flux was inappropriate in that particular circumstance and others. Kioussis states that the Jaumann stress "rate" (stress flux) is not applicable to materials exhibiting kinematic hardening. Whether this conclusion is verified or if the constitutive model assumed is at fault remains to be seen.

Since there is a wide variety of choices for the stress flux, it is omnious to presume that one must be selected for each combination of constitution and loading trajectory. Eringen(80) offers seven permutations. It is notable that the property of objectivity is distributive to transformation so new versions can be formed by adding objective tensors or groups.

| | | |
|---------|----------|---|
| | JAUMANN | $\dot{\sigma} = \dot{\sigma} + \sigma W - W\sigma$ |
| STRESS | OLDROYD | $\dot{\sigma}^* = \dot{\sigma} - \sigma \nabla V - \nabla V \sigma$ |
| FLUXES: | TRUEDELL | $\dot{\sigma}^\dagger = \dot{\sigma} - \sigma \nabla V - \nabla V \sigma + \sigma \nabla \cdot V$ |
| | ERINGEN | $\hat{\sigma} = \dot{\sigma} + \nabla V \sigma - \sigma \nabla V$ |

$\pm \sigma D \dots etc.$

The basic set of stress fluxes are built from grad V , and stem from the relation between material and moving coordinate frames. The need arises when incorporating stress rate (material derivative) into the constitutive relation because stress rate is not inherently objective. This usually amounts to a sort of Boussinesq approximation in that grad V is ignored in the momentum equation but included in the constitutive statement. Thus the momentum equation becomes:

$$\nabla \cdot \sigma = \rho g k \dots \quad \dot{V} = \frac{\partial V}{\partial t} + V \cdot \nabla V = 0$$

In order to lay a groundwork for the new stress fluxes, the following is a condensation of Truesdell(77) II chapters 5-11.

$$\nabla V = G = D + W \quad \text{velocity gradient}$$

$$\nabla x = F = RU = VR \quad \text{deformation gradient}$$

polar decomposition..rotation tensor, RH stretch tensor
LH stretch tensor

$$G = \dot{F}F^{-1}$$

$\{ V \}$ is frame indifferent $F U \& R$ are not $\}$

$$V = RUR^T$$

$$J = \det U = \det V \quad \text{jacobian}$$

$$U^2 = FF^T \quad \& \quad V^2 = FF^T$$

R - carries principal axes of strain in X
into principal axes of strain in x

if $R = I$; $U = V \Rightarrow$ pure stretch

$$W = \dot{R}R^T + \frac{1}{2}R(\dot{U}U^{-1} - U^{-1}\dot{U})R^T$$

spin components from polar decomposition

$$D = \frac{1}{2}R(\dot{U}U^{-1} + U^{-1}\dot{U})R^T$$

deformation rate components from polar decomposition

if Q orthogonal tensor between frames

$$D^* = Q D Q^T \quad \# \text{ (hence objective)}$$

$$\text{but: } W^* = Q W Q^T + A$$

$$A = \dot{Q}Q^T \quad \text{is the spin of frames joined by } Q$$

relative to one another

so that the asterik deformation rate is frame indifferent while the asterik spin is the original plus the relative.

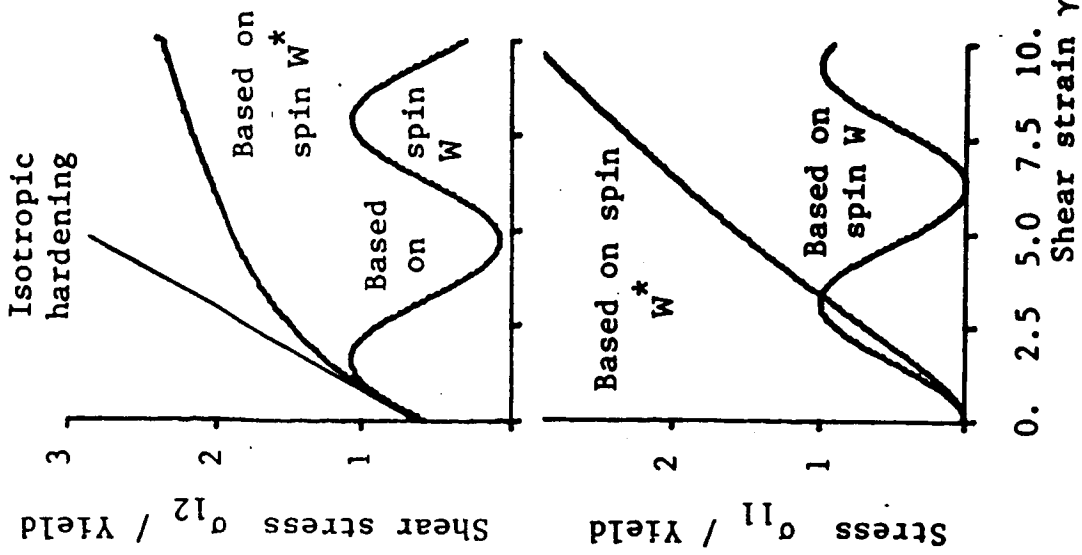


FIGURE 3 LEE STRESS FLUX

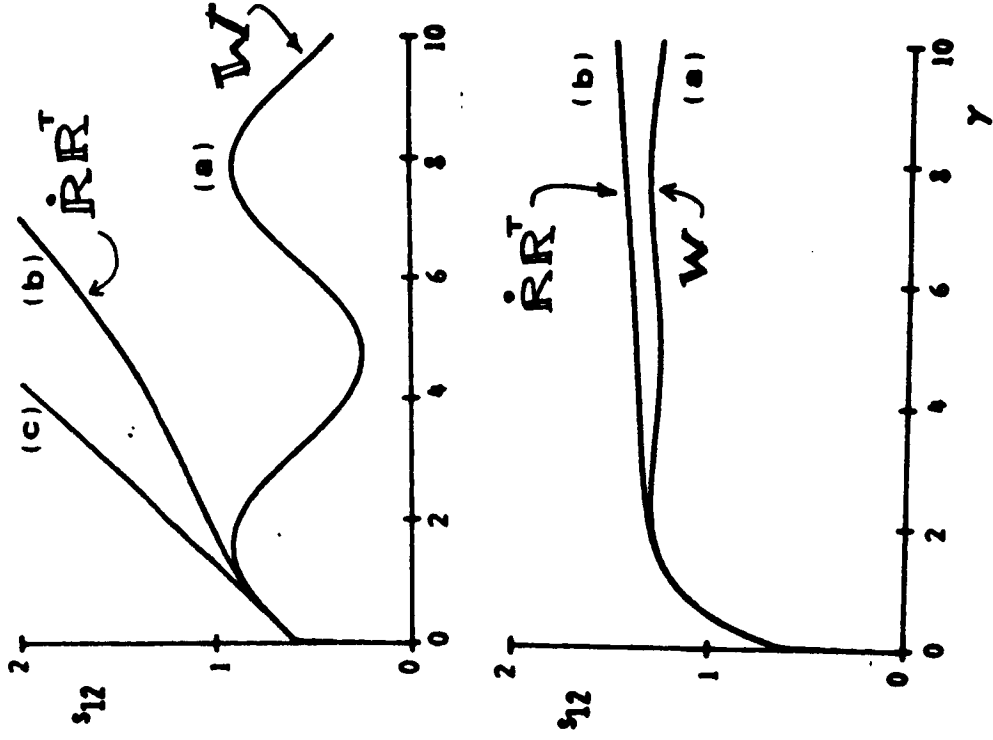


FIGURE 4 DAFALIAS STRESS FLUX

STRESS POWER

In a general thermodynamic description of a material stress power (nominally $\sigma \cdot D$) and mass density are related by the temperature variable between the "energy" and the "state" equations. The granular formulations while sometimes alluding to "adiabatic," invariably decouple the equations by removing any temperature sensitivity from the equations for energy and state. They are thus left related only by:

$$\dot{e}_v = - \frac{1}{\rho} \frac{D\rho}{Dt} = \text{tr } D = \nabla \cdot v$$

Density is occasionally coupled to pressure ($1/3 \text{ tr } \sigma$) but the comparison is invariably on an integral, time independent basis (SR vs e_v).

Stress power and density are allied in that they appear in the coefficients of the full constitutive model..[]...Scott(84) following the general 10 coefficient model of Truësdell(55); basically this is a polynomial formulation in σ and D linearized in σ and D alone but including the components of $\sigma \cdot D$. There is perhaps a problem with this formulation for certain finite strain situations; consider the development below and notice that the Jaumann Quandary also becomes embroiled here for integrals over strain.

$$P = \frac{D}{Dt} \int \sigma \cdot dE \quad [\text{energy/volume/time}]$$

(cf: $\text{tr } \sigma D = p \text{tr } D + \text{tr } \sigma^* D^*$) nominal stress power

$$P = \sigma \cdot D)_f - \sigma \cdot D)_i + \int_{E_i}^{E_f} \frac{D\sigma}{Dt} \cdot dE$$

$$\dot{\sigma} = \hat{\sigma} + \sigma \Omega - \Omega \sigma$$

stress flux.....see J.Q.

$$[]_1 \Pi + []_2 D + []_3 \sigma \quad \text{constitutive}$$

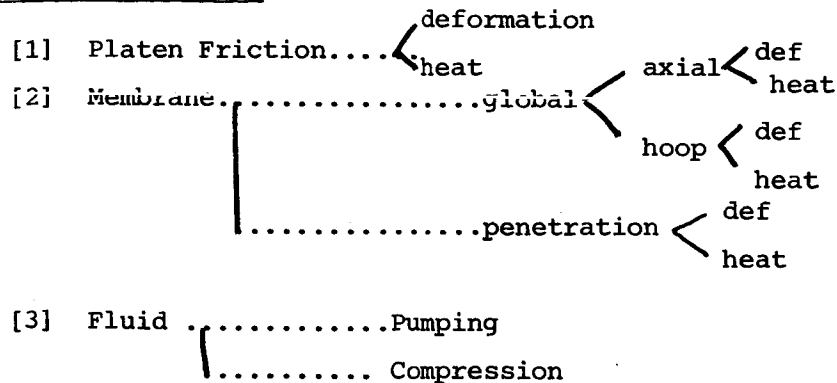
Source Power: Interstitial + Gravity+ Confinment+ Sink

$$F \cdot V = \int P dv + Mg z + \int \sigma A dr + S$$

..... kinetic energies being explicitly neglected.....

$S \triangleq$ power sink terms both potential and dissipative

Power Sink Candidates:



Beyond the normal component for the encroaching platen which is the ultimate power source, the boundary working rate includes the following, pumping and compression for the confining fluid, membrane stretching and penetration, and platen shear working rate. There is also the compression and pumping losses in the pore fluid, movement of the center of gravity (if $g \neq 0$) and last but certainly not least the interstitial working rate of the granular medium.

Another view of stress power is that commonly taken by the fracture mechanists, which is to assess damage as a quantitative measure of the "sunked" power; (ie the non elastic effects ..both the membrane and undrained fluids could also exhibit reversible compression) and which appears in various forms in the coefficients of the constitutive relation. The fabric of the material is damaged in a way not delt with specifically , but its constitution changes in proportion to the sunked power. Kachanov(86) The use is sometimes made of a quantity termed, creep dissipation density: $\dot{\sigma} D$

In the most general approach to this sort of analysis, Dunn & Serrin (85) introduce the interstitial working rate as:

$$\sigma \cdot \nabla V = \sigma \cdot (D + W)$$

Both the creep dissipation and the interstitial working open the Jaumann Quandary once again.

STRAIN DEFINITION AND RESOLUTION

This project has as a bounding condition a steadily encroaching platen with a centering force provided by a porous stone centrally located and of relatively small radius. The platen is nominally frictionless, hence at the moving platen boundary;

$$\dot{\epsilon}_{zz} = C, \quad \dot{\epsilon}_{rr} = \dot{\epsilon}_{\theta\theta} = \text{full slip} .$$

That is the rates are prescribed independently of the rate behaviour brought into the motion by the constitution. Ultimately it is envisioned that the surface response will be sought as a sequence of optical images; optical segments will be identified and tracked. Particularly the images formed from the outer surface of the cylindrical surface. Subsequently an association will be made with the strain field and hence with the analytically generated strain predictions from the integrations of a continuum model.

The following discussion is a consideration of the implications to the theoretical modeling of the anticipated order of magnitude of the movement and necessary transformations to establish a relation with optical displacements. This is an important precursor to the detailing of the constitutive model and its numerical counterpart. The intent is to identify and highlight the variety of "strains" without resolving them all. This search is the prolegomenon to relating optical displacement, optical strain, computed strain, and true strain. That is the initiation of the correct processing algorithm and calibration requirements.

Rates enter the specification from both the strobe nature of the optical technique and from the material constitution and loading trajectory (viz: constant strain rate); the proper phasing of these three should be included in the design of the final experiment. Rotation of material lines, spin of embedded granules as associated with "bulging and lumping" (see Thin Shell section) is crucial as they will add to the distortion and must be compensated or the optical scheme must disallow these measurements automatically. As is discussed in the next section, the constitutive theory will not model the local surface phenomena, lumps, and probably will not predict the global surface phenomena, bulges.

Some learning about evolution from the prototype experiments, may provide the prophylactic scheme for rejection of data during a surface aberration. For example; apparently local failures precede global failure, and at the least their growth is enhanced by global failure. Hence the growth of local failure could predict location and age of global failure.

In Terzaghi & Peck (60) (pp109) after giving a lengthy exposition the author adds "...from slow tests very much smaller values are obtained." In any venture of this sort the rate terms from the full constitution should be considered, if in no more detail than as order of magnitude studies of dimensionless weightings. Even the integral strain rate varies from its nominal value;

$$\dot{\epsilon} = \dot{\epsilon}_{nom} (l/l_0)$$

and the time rate for even increments of strain in that same sense;

$$\Delta t = \left(1 - \frac{tV_{\dot{\epsilon}}}{l_0}\right) \frac{1}{\dot{\epsilon}_{MP}(\Delta \epsilon)}$$

It is also necessary to distinguish between a change in the time scales of response and true creep, because the local strain histories are quite different after appreciable strain.

$$\begin{array}{c} \text{STRESS Response} \\ \frac{\partial \sigma}{\partial t} \end{array} = \begin{array}{c} \text{CONSTITUTION} \\ \frac{\partial \sigma}{\partial \epsilon} \frac{\partial \epsilon}{\partial t} \end{array} + \sum \begin{array}{c} \text{STRAIN signal} \\ \frac{\partial \sigma}{\partial x} \frac{\partial x}{\partial t} \end{array}$$

Collecting the notation from Eringen(80):

Lagrangian strain-- $E_{kl} = \tilde{E}_{kl} + \frac{1}{2}(\tilde{E}_{mk} + \tilde{R}_{mk})(\tilde{E}_{ml} + \tilde{R}_{ml})$

Eulerian strain- - $e_{kl} = \tilde{e}_{kl} + \frac{1}{2}(\tilde{e}_{mk} + \tilde{r}_{mk})(\tilde{e}_{ml} + \tilde{r}_{ml})$

deformation gradients - - $\nabla U = \tilde{E} + \tilde{R} = F$
 $\nabla u = \tilde{e} + \tilde{r}$

velocity gradient - - $\nabla V = D + W = \text{deformation rate} + \text{spin}$

with $\tilde{}$ indicating infinitesimal quantities of strain and rotation

Hence vanishing infinitesimal strain are not sufficient to specify rigid deformation; infinitesimal strain is not a strain measure except under "infinitesimal" conditions, for which Eulerian and Lagrangian strains are identical.

$$\dot{E} = \frac{\partial E}{\partial t} \quad \& \quad \dot{e} = \frac{\partial e}{\partial t} + v \cdot \nabla e$$

$$\dot{E} = D \dots \dots \dots \text{infinitesimal deformations}$$

$$\dot{e} \approx D \quad \text{if } W \ll O(D)$$

$$\boxed{\dot{e} = D - e \nabla V + \nabla V e}$$

it is also interesting that $J \approx 1 + \text{tr } \tilde{e}$

THIN SHELL CONSIDERATIONS

There is an interesting possibility that a triaxial sample with a highly penetrated membrane exhibits a thin shell response for certain ranges of loading. The proximity of a tension element (membrane) and a compression element (granules) linked with intergranular and membrane penetration friction forces sets the scene for thin shell behaviour. (see Figure 5) Specifically the interest is only in the onset of buckling and post-buckling regimes.

The interest in making these considerations arises for two reasons. First because of the appearance in testing of 3-D surface patterns which persist and grow in a nonhomogeneous way. Secondly because it is crucial to the rational model that in the region where theoretical model meets measurement there is a special physics. High penetration, large friction coefficient and their exponential coupling via membrane tension will allow the membrane to dominate the stress power, locally in a layer $O(d)$ thick. The suggestion of patterns is nicely revealed by the experimental work with pressure and axially loaded thin metal cylinders; Schnell(60), Figure 5.

Subject to extreme membrane penetration from high confinement there is in the early stages of loading a thin shell behaviour. The shell fails leaving surface irregularities in the form of lumps, bumps and pimples. It is important to note that preliminary calculations show the effect to be strictly superficial to the total loading-deformation behaviour, but as the loading progresses the surface irregularities grow and become exaggerated. In fact the growth is preferential with nonuniform geometry changes in that the "bulge" region irregularities show greatly accelerated growth. The local scale seems to predict and interact with the larger scales of deformation that are referred to as "bulge".

These phenomena are shown on the length scales caricature; Figure 6, and are accompanied by a typical set of values as Figure 7, all related to the bead diameter. The first scale is a measure of the extent to which beads penetrate the confining membrane, with low penetration requiring a value $O(1)$ and is a measure of the angle through which the membrane turns in traversing a bead. Somewhat arbitrarily a membrane with $t/d O(0.1)$ will be termed thin and one with $t/d O(1)$ will be termed thick.

As with a very uniform shell of homogeneous material, imperfections will greatly effect the load that marks catastrophe. (see Figure 10) Of course in the preparation of samples of material for a triaxial test leaves many fabric anomalies at the surface. These sites will

undoubtedly provide imperfections for buckling, and encourage premature failure. After failure these sites are marked with continual growth of vestigial lumps, ridges and depressions.

The presumption is that under cyclic loading the shell phenomenon would not reappear as the residual wrinkles would still be present. However they would without a doubt continue to grow monotonically under all cyclic loading being true catastrophe products and irreversible to the loading that produced them. Ironically, the postulate is that shellness is related to thin membranes; those with less internal bending stresses. The simple concept that hoop stress varies as the reciprocal of thickness must be viewed with askewance at high membrane strain. The extreme rise in modulus of elasticity with strain could cause thin membrane strains to be less than thick membrane strains; see Figure 11.

Under the assumed sequence of membrane penetration preceding axial load and the subsequent formation of an unbonded, friction linked shell; it is perhaps plausible that the shell would resemble the situation in a reinforced concrete shell. Seide(81) gives a broad survey, and using his equations as an estimation tool with the property values for latex rubber gives the results in Figure 9. The estimates are presumably lower bounds ; but as this shell does not have a distinct thickness or homogeneity of moduli there is no use to pursue this analog any further. The conclusion however is clear. In Figure 9 the "P" is the critical value of external pressure for buckling under that loading alone and the " σ_c " for axial stress alone; since both are typically present it might be of value to use Seide's combined loading figures, but to this level of approximation it is not helpful beyond the observation that critical axial loads would be reduced considerably. As an example consider the case of $t/d = 3.3\text{mm}$. the critical pressure of 0.01 psi must be related to the confinement minus the pore pressure (or $1/3 \text{ tr } \sigma_c$) and the total axial load would be $2\pi R t \sigma_c - 1.8 \text{ Lbf}$. The figure is intended to be schematic and does not show penetration which is assumed, $t/d = 0.1$.

STRESS OFFSETS

| | |
|------------------|-----------------|
| INCREMENTAL..... | LOCAL |
| DEVIATORIC..... | TRACE |
| EFFECTIVE..... | PORE PRESSURE |
| BACK STRESS..... | CENTER OF YIELD |
| (SHIFT STRESS) | SURFACE |

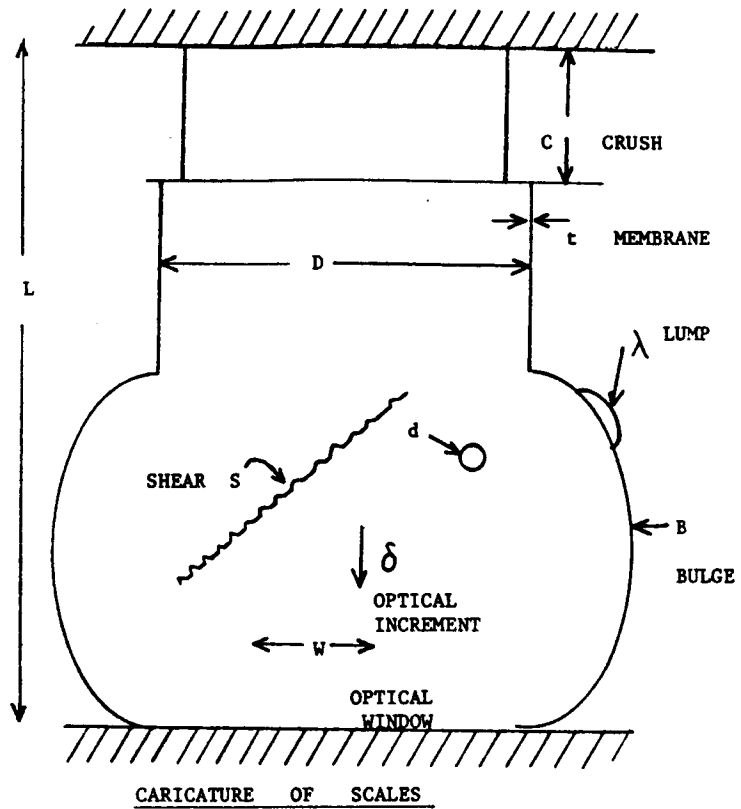


FIGURE 6 LENGTH SCALES

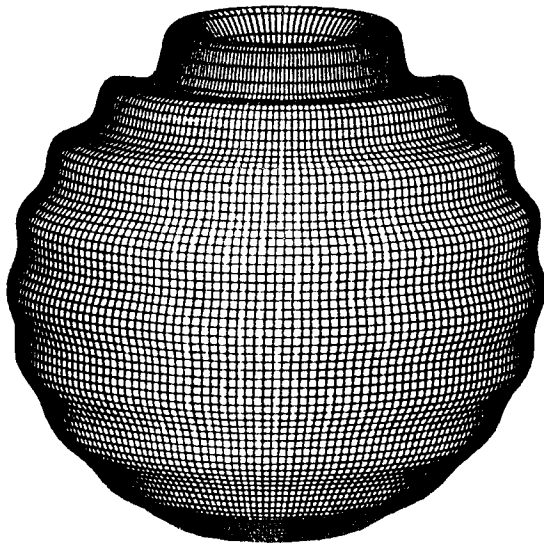
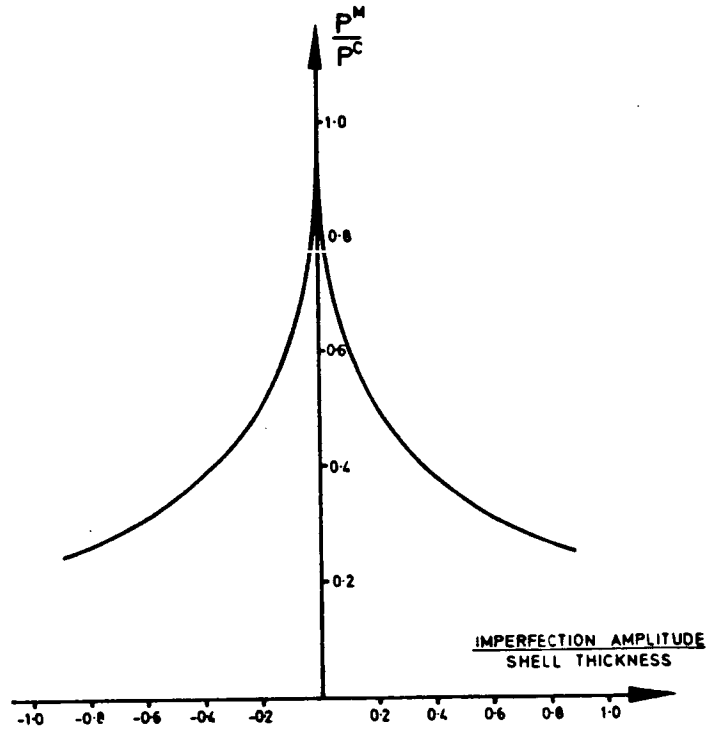


FIGURE 12 BUCKLED THIN SHELL

| | | |
|-------------|---|-----|
| t/d | - | 0.1 |
| λ/d | - | 5 |
| B/d | - | 25 |
| D/d | - | 25 |
| L/d | - | 35 |
| δ/d | - | 1 |
| w/d | - | 10 |

TYPICAL SCALING
 $d = 3\text{mm}$

FIGURE 7

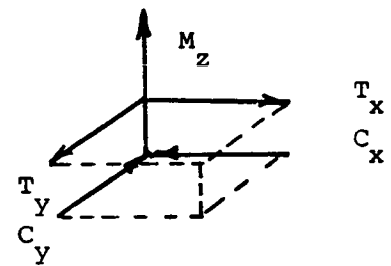
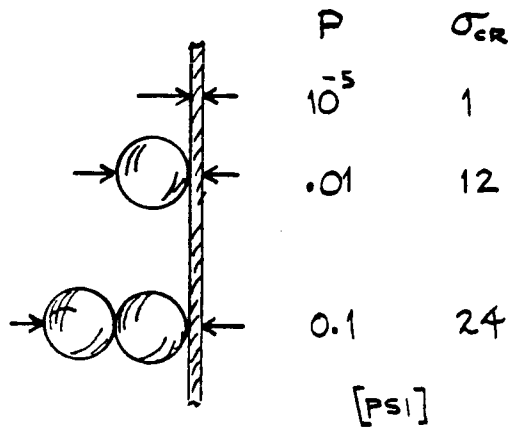


$$P = \frac{1}{4(1-\nu^2)} E \left(\frac{t}{R}\right)^3$$

$$\sigma_{CR} = \frac{1}{\sqrt{3(1-\nu^2)}} E \left(\frac{t}{R}\right)$$

PREMATURE CYLINDER BUCKLING

FIGURE 10



MEMBRANE-GRANULE FRICTION

COUPLED COMPOSITE

FIGURE 8

$$E = 140 \text{ [psi]} ; \quad \nu = 0.5$$

ESTIMATES OF CRITICAL EXTERNAL PRESSURE
AND AXIAL STRESS

FIGURE 9

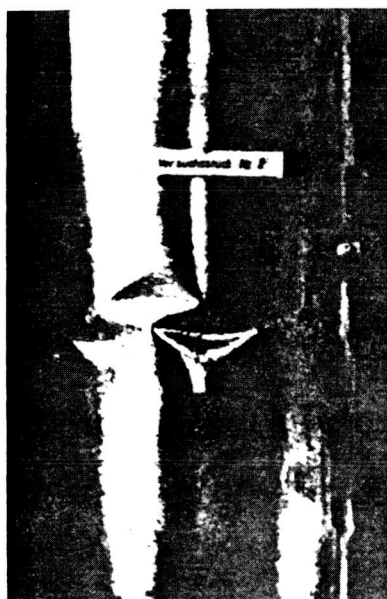


Ohne Innendruck $\bar{p} = 0$



Mit Innendruck $\bar{p} = 0,66$

Orthotroper Zylinder $\left\{ \begin{array}{l} \tau \\ \sigma \end{array} \right. = 290$



Ohne Innendruck $\bar{p} = 0$



Mit Innendruck $\bar{p} = 2,38$

THIN SHELL FAILURE PATTERNS CIRCULAR CYLINDER

FIGURE 5

NUMERICAL APPROACH

The ultimate source for the sequence of programs given the generic title MICROFEM is Chapter 24 (by R.L. Taylor) of the classic text by Professor Zienkiewicz, The Finite Element Method, McGraw (1982). The version produced in this work is a direct ancestor of several versions from the students of Professor Ko at the University of Colorado. Most recently DENISE.FTN by Garrett Denise, (MSFC name). All are application oriented and have substantial differences, but the general solving subroutines are essentially unchanged. The most important feature being the Lade-Nelson constitutive model, added to the framework of the ultimate source. The next page is dedicated to listing, locating and typing the subroutines in this code.

The program (MAIN) drives 26 subroutines and 1 function. After an initial commitment to nodalization, three subroutines are dedicated to checking size compatibility with the local environment: the current levels set are well below the capabilities of the local PE 3250 on which the program is installed. The setup is done by a menu driven query in INPUT; this drives on command turning on of flags(1,7,8,9,10), direct entering of acceleration of gravity (11), calling other subroutines(2,3,4,5,6,12) and exit(13). FORCE and AXIFORCE are used to commit the external loading; confining and axial respectively (6,12). Stress and strain at "Gauss points" is output from RESPØ1 which is called from several places in other subroutines via RESPON; the usual sequence is: LOAD,SOLVER,RESPON (RESPØ1).

The local name of MICROFEM is MGMFEM.FTN. It has been given a command file MGMFEM.CSS to drive it by its own name. Further a manual has been produced to provide some detail of the source and evolution for the MICROFEM family, details of operation, and coding flow to assist in modification. The manual includes; explicit startup instructions, hardcopy of the screens that appear during a run (ie: menus, prompts for input, mirrored array generation, and output), a subroutine listing with a brief description of utility, a subroutine level flow chart with ties to the data I/O points. There is also some command level instruction for generating a LOG file of an interactive session, and the code for the autorun command file.

The earlier versions of the code were run batch-style and setup from a data file. They have been retained locally as AXI.FTN, BI.FTN and DENISE.FTN. Also the BASIC program Capmodel has been converted from HP-BASIC to BASICA for the AT driving an HP plotter. There are 5 model stables in the MICROFEM code and 4 remain unused. One of the primary goals of the numerical phase of MGM analysis should be to populate those stables so that several types of constitution could be run with a single initialization.

ORIGINAL PAGE IS
OF POOR QUALITY

SUBROUTINE LISTING: MGMFEM.FTN

| LOCATION | TYPE | NAME | ARGUEMENTS |
|----------|------|---|--|
| 140 | * | SUBROUTINE INITIAL | (IE, IX, ID, D, X, XL, UL, |
| 141 | | 1 NNP, NEL, NMAT, NDIM, NEN, NEN1, NDOF, STRESS, PA, XKUR, XN, XNI, | |
| 142 | | 2 CL, PC, XM, ETA1, S1, S2, T1, T2, W1, W2, Q1, Q2, SK, BK, UBK, R, JDIAG, | |
| 143 | | 3 NSEC, NEG, NAC, IFAIL, TOL, DENSIT, NSTEP, NITER, | |
| 144 | | 4 PRFP, PRFC) | |
| 343 | # | SUBROUTINE INCLQAD | (IE, IX, ID, D, X, F, XL, UL, NNP, NEL, |
| 344 | | 1 NMAT, NDIM, NEN, NEN1, NDOF, STRESS, PA, XKUR, XN, XNI, CL, PC, | |
| 345 | | 2 XM, ETA1, S1, S2, T1, T2, W1, W2, Q1, Q2, SK, BK, UBK, R, JDIAG, NSEQ, | |
| 346 | | 3 NEG, NAD, IFAIL, TOL, NUMINC, DISP, PRFP, PRFC) | |
| 485 | * | SUBROUTINE CHKSTR | (I, J) |
| 509 | * | SUBROUTINE IZERO | (I, NUM) |
| 516 | * | SUBROUTINE RZERO | (A, NUM) |
| 523 | * | SUBROUTINE INPUT | (IE, D, IX, ID, X, F, IXL, XL, IDL, FL, MN, NNP, NEL, |
| 524 | | 1 NMAT, NDIM, NEN, NEN1, NDOF, PA, XKUR, XN, XNI, CL, PC, XM, ETA1, S1, | |
| 525 | | 2 S2, T1, T2, W1, W2, Q1, Q2, TOL, NUMINC, DENSIT, NSTEP, NITER) | |
| 612 | * | SUBROUTINE COORD | (X, XL, MN, NNP, NDIM, IPRT, IERR) |
| 679 | * | SUBROUTINE ELTOP | (IX, IXL, NEL, NEN, NEN1, IPRT, IERR) |
| 735 | * | SUBROUTINE FIXITY | (ID, IDL, NNP, NDOF, IPRT) |
| 801 | * | SUBROUTINE FCRCE | (F, FL, ID, NNP, NDOF, IPRT, IERR, NUMINC) |
| 859 | * | SUBROUTINE AXIFORCE | (IX, IXL, F, FL, X, XL, NEL, NEN, NEN1, NDIM, NDOF, NNP, |
| 860 | | 1 IPRT, IERR, NUMINC) | |
| 979 | # | SUBROUTINE MATLIB | (M, IE, D, NGK, NGS, NMAT, IPRT, IERR, PA, XKUR, |
| 980 | | 1 XN, XNI, CL, PC, XM, ETA1, S1, S2, T1, T2, W1, W2, Q1, Q2) | |
| 1010 | # | SUBROUTINE MATO1 | (M, IE, D, NGK, NGS, NMAT, IPRT, PA, XKUR, XN, XNI, |
| 1011 | | 1 CL, PC, XM, ETA1, S1, S2, T1, T2, W1, W2, Q1, Q2) | |
| 1128 | \$ | SUBROUTINE PROFIL | (IX, ID, JDIAG, NNP, NEL, NEN, NEN1, NDOF, NST, |
| 1129 | | 1 NAD, NEG) | |
| 1170 | \$ | SUBROUTINE STIFF | (IE, D, IX, X, ID, XL, SK, JDIAG, BK, UBK, NNP, NEL, NMAT, |
| 1171 | | 1 NEN, NEN1, NDIM, NDOF, NEG, NSEQ, NAD, DSTRES, PA, XKUR, XN, XNI, CL, PC, | |
| 1172 | | 2 XM, ETA1, S1, S2, T1, T2, W1, W2, Q1, Q2, IFAIL, ITAG, PRFP, PRFC) | |
| 1203 | \$ | SUBROUTINE STIF01 | (IE, D, IX, X, ID, XL, SK, JDIAG, BK, UBK, NNP, NEL, |
| 1204 | | 1 NMAT, NEN, NEN1, NDIM, NDOF, NEG, NSEQ, NAD, STRESS, PA, XKUR, XN, | |
| 1205 | | 2 XNI, CL, PC, XM, ETA1, S1, S2, T1, T2, W1, W2, Q1, Q2, IFAIL, ITAG, | |
| 1316 | # | SUBROUTINE GAUS01 | (L, LINT, SG, TG, WG) |
| 1343 | # | SUBROUTINE SHAP01 | (S, T, XL, NDIM, NEN, SHP, B, DETJ) |
| 1368 | * | SUBROUTINE ADDSTF | (SK, LM, BK, UBK, JDIAG, NSEQ, NAD, NEG) |
| 1384 | # | SUBROUTINE LOAD | (ID, F, R, NNP, NDOF, NEG) |
| 1395 | # | SUBROUTINE SOLVER | (BK, UBK, R, JDIAG, NEG, NAD, IFLAG) |
| 1438 | \$ | SUBROUTINE DLADE | (STR1, STR2, STR3, STR4, PA, KUR, N, NI, CL, PC, |
| 1439 | | 1 M, ETA1, S1, S2, T1, T2, W1, W2, Q1, Q2, IFAIL, DEP, AP, AC, FP, FC) | |
| 162 | # | SUBROUTINE RISEC | (A, B, D, FP, PA, C, D, ER, X, IFLAG) |
| 1647 | # | SUBROUTINE RESPON | (IE, D, IX, X, ID, F, XL, UL, R, NNP, NEL, NMAT, NEN, |
| 1648 | | 1 NEN1, NDIM, NDOF, NSEQ, NEG, DDSTRE, STRESS, PA, XKUR, XN, XNI, | |
| 1649 | | 2 CL, PC, XM, ETA1, S1, S2, T1, T2, W1, W2, Q1, Q2, PRFP, PRFC, IFAIL) | |
| 1699 | # | SUBROUTINE RESP01 | (IE, D, IX, X, F, XL, UL, NNP, NEL, NMAT, NEN, NEN1, |
| 1700 | | 1 NDIM, NDOF, DDSTRE, STRESS, PA, XKUR, XN, XNI, CL, PC, XM, ETA1, | |
| 1701 | | 2 S1, S2, T1, T2, W1, W2, Q1, Q2, PRFP, PRFC, IFAIL) | |
| 1922 | \$ | SUBROUTINE PSTRES | (SIG, PSIG) |
| 1639 | # | FUNCTION DOT | (A, B, N) |

* - - - SETUP
- - - GENERAL SOLVING
\$ - - - MODEL RELATED

CONCLUSIONS & RECOMMENDATIONS

The Jaumann Quandary has been laid out in some detail and put in perspective as a "state of the art" question in rational mechanics. The resolution of stress flux "choice" is pivotal to any confidence in numerical modeling beyond the well established realms. A clear definition has been given for stress-power in the incremental sense. Apparently the impact of the stress-flux on this integral has not been realized before. The reoccurrence of the J.Q. has been shown at several places in the Scott(84) constitutive relation.

The analytic path from optical displacement to the "true" strain(s) has been covered in some detail, but optical displacement is not yet resolved to numerical (FE) strain which will vary somewhat with specific algorithm.

A close inspection should be made of the optimization process for t/d ; the strategy to minimize membrane thickness alone may be "faulted". First: it is very important to control vestigial formations if surface strains are to be measured.

Second: there is ultimately a thinness limit to lowered hoop stress established by the onset of increased modulus of elasticity.

Third: the optical detection and selection process is much more robust than originally envisioned; and able to handle considerably higher t/d than 0.1.

In light of the thin shell physical model presented above, the conclusion is that a thin membrane ($t/d \approx 0.1$) may encourage the production of vestigial lumps on the sample surface. These formations, while not changing the gross behavior of the testing may cause considerable interference with attempts to measure optical surface displacements.

Hence the maximum t/d is encouraged which will still permit optical processes to remain error-free in following red-granule trajectories. Whether t/d can be made to approach $O(1)$ within the constraints of low confining pressure, minimum optical resolution and optical transparency remains to be seen.

An improved version of "MICROFEM" has been produced; MGFEM.FTN, which resides on the Fluid Dynamics Branch Perkin-Elmer 3250. It is fully interactive and can be flagged to mirror entry, output to screen or printer, reinput data, and so on. The data entry necessary for a run has been reduced by eliminating features not pertinent to the problem at hand; ie: RPM, other geometries, multiple material types, etc), but the acceleration of gravity has been explicitly added as input. The following features still need to be modified; the code is still time insensitive, the loading is limited to stress initiation, the model stable has only Lade-Nelson, and many options for post-processing need to be implemented for a satisfactory analysis tool.

REFERENCES

- [1] Coleman, B.D. & M.L. Hodgdon, " On Shear Bands in Ductile Material", Arch. Rat.Mech.Analy.",v.88n.4 (1985).
- [2] Dafalias, Y.F., "Corotational Rates for Kinematic Hardening at Large Plastic Deformations", Trans ASME J.Appl.Mech. v.50,561, (1983).
- [3] Dunn, J.E. & J. Serrin, "On the Thermomechanics of Interstitial Working", Arch.Rat.Mech. Analy., v.88 n.2 (1985).
- [4] Faruque, M.O. & C.S. Desai, " Implementation of a General Constitutive Model for Geological Materials", Int.J.Num.Analy.Meth.Geomech., v.9,415, (1985).
- [5] Hettler, A. & I. Vardoulakis, "Behavoir of Dry Sand Tested in A Large Triaxial Apparatus", Geotechnique,v.34, n.2 (1984).
- [6] Kachanov, L.M., Introduction to Continuum Damage Models , Nijhoff, (1986).
- [7] Kioussis, P.D., G.Z.Voyiadjis & M.T. Tumay, " A Large Strain Theory for the Two-Dimensional Problems in Geomechanics", Int.J.Num.Analy.Meth.Geomech., v.10,n.1, (1986).
- [8] Koiter, W.T., Proc. I.U.T.A.M. Symposium, Theory of Thin Elastic Shells, (W. Schnell, "On the stability of Pressurized Thin Cylinders Under Longitudinal Loading" (in German)), North-Holland,Delft ,(1960).
- [9] Lade, Poul V.& R.B. Nelson, "Incrementalization Procedure for Elasto-Plastic Constitutive Model with Multiple, Intersecting Yield Surfaces", Int.J.Num.Analy.Meth.Geomech.,v.8,311,(1984).
- [10] Lee,E.H.. R.H Mallett & T.B. Wertheimer," Stress Analysis for Anisotropic Hardening in Finiet-Deformation Plasticity", Trans. ASME J.Appl.Mech., v.50, 561, (1983).
- [11] Loret, B. & J.H. Prevost, " Accurate Numerical Solutions for Drucker-Prager Elastic-Plastic Models", Comp.Meth.Appl. Mech.Engr., v.54, n.3, (1986).

- [12] Molenkap, F., " Comparison of Frictional Material Models with Respect to Shear Band Initiation", *Geotechnique*, v.35, n.2 (1985).
- [13] Prevost, J.H., " Constitutive Equations for Soil Media", in (Martin, J.B., Numerical Methods in Geomechanics, Reidel, 1982), (1981).
- [14] Seide, P., "Stability of Cylindrical Reinforced Concrete Shells" in (Popov, E.P., Concrete Shell Buckling, SP-67, ACI, Detroit), (1981).
- [15] Siriwardane, H.J., & C.S Desai, "Computational Procedures for Non-linear Three Dimensional Analysis of Advanced Constitutive Laws", *Int.J.Num.Analy.Meth.Geomech.*, v.7,143, (1983).
- [16] Vardoulakis, I., "Bifurcation Analsis of the Triaxial Test on Sand Samples", *Acta Mechanica*, v.32, 35. (1979)
- [17] (1981) "Constitutive Properties of Dry Sand Observable in the Triaxial Test", *Acta Mechanica*, v.38,219.
- [18] (1983) "Rigid Granular Plasticity Model and Bifurcation in the Triaxial Test", *Acta Mechanica*, v.49,57.
- [19] (1985) "Stability and Bifurcation of Undrained Plane Rectilinear Deformations on Water-Saturated Granular Soils", *Int.J.Num.Analy.Meth.Geomech.* v.9 ,399, (1985).
- [20] (1985) & B. Graf, " Calibration of Constitutive Models for Granular Materials Using Data from Biaxial Experiments", *Geotechnique*, v.35,299.
- [21] Zampelli, S.P. & S. Sture, Behavoir of Granular Cohesionless Soils at Very Low Effective Stress Levels, Final Technical Report to Dr. N.C. Costes NASA/MSFC, NAS8-35668, MSFC, (1985).